UvA-DARE (Digital Academic Repository)

epsilon-delta phase transition of nitrogen and the orientational behavior of the second-order transition within the delta phase: A Monte Carlo study at 7.0 GPa.

Mulder, A.; Michels, J.P.J.; Schouten, J.A.

Download date: 23 Nov 2017

ε-δ phase transition of nitrogen and the orientational behavior of the second-order transition within the δ phase: A Monte Carlo study at 7.0 GPa

A. Mulder, J. P. J. Michels, and J. A. Schouten

Van der Waals-Zeeman Institute, University of Amsterdam, Valckenierstraat 65, 1018 XE Amsterdam, The Netherlands

Monte Carlo simulations have been performed with an improved nitrogen-nitrogen potential at 7.0 GPa, to study the behavior near the ε-δ phase transition, to calculate the vibrational frequencies in the δ phase, and to examine the second-order phase transition within the δ phase. The ε-phase structure transformed to the δ-phase structure at 140 K, whereas the δ-phase structure is metastable below this temperature. The second-order transition could be detected in several ways. At high temperature the orientational behavior of all molecules is highly dynamical with weakly preferred orientations. At the second-order transition the molecules at the *disk* sites become localized with different orientations, whereas the orientational behavior of the molecules at the *sphere* sites does not change. The localization causes the frequency of the disk sites to split with an intensity of 1:2, and influences the frequency of the sphere sites. The frequency behavior calculated with this model system resembles the experimental behavior. Additional calculations revealed that the anisotropic energy term as well as the Coulomb term of the intermolecular potential influence not only the stability of the ε-phase structure, but also the orientational behavior, and thus the nature, of the second-order phase transition. [S0163-1829(98)07813-8]

I. INTRODUCTION

The phase diagram of nitrogen exhibits several solid phase transitions, which involve an orientational order-disorder transition as well as structural changes (Fig. 1). Up to about 0.4 GPa the β phase[1–5] (disordered hcp) transforms at low temperature to the α phase[2,3,6–9] (ordered fcc), whereas at higher pressures up to 2.0 GPa the β phase transforms to the γ phase[3,6,10] (ordered tetragonal).

At still higher pressure the ε-δ transition is found, which has been examined with x-ray diffraction[11,12] and Raman scattering.[13,14] The δ phase ($Pm3n$) (Refs. 11, 12, and 15) is the orientationally disordered phase. Not all molecules exhibit the same disorder: the molecules at the corners and the center of the cubic unit cell of the δ phase are *spherically* disordered, whereas the molecules in the faces of the cell are *disklike* disordered [Fig. 2(a)]. Although the nature of the orientational disorder could not be experimentally established,[15] computer simulations[16,17] indicate it is highly dynamical. The unit cell of the ε phase[11] [$R\bar{3}c$, Fig. 2(b)] is a trigonal distortion of the unit cell of the δ phase: the δ-ε transition can be thought of as taking place through a change in the cell angles of a few degrees, $\Delta\alpha$, depending on pressure and temperature, together with a small displacement, Δx, and orientational ordering of the molecules. The center and corner molecules, which can be identified as the spherically disordered molecules in the δ phase, align along the (111) body diagonal. The face molecules, which can be identified as the disklike molecules in the δ phase, align at $\varphi_d = 45°$ in the plane of the disk with respect to the axis normal to each face, and at an angle θ_d with the normal of the plane of the disk. The angle θ_d depends on the angles of the unit cell. An extensive Raman study performed by Scheerboom and Schouten[18,19] revealed a second-order transition within the δ phase. Figure 3 shows the behavior of the frequencies

of the spheres (ν_1) and the disks (ν_2) at 5.9 GPa. This behavior has been explained as follows: at the structural transition to the δ phase the molecules obtain some orientational freedom and liberate around a few equally probable orientations: orientational localization (δ_{loc}). On further heating the rapid decrease of ν_1 is caused by a cascade process in which this localization vanishes rapidly. The end of
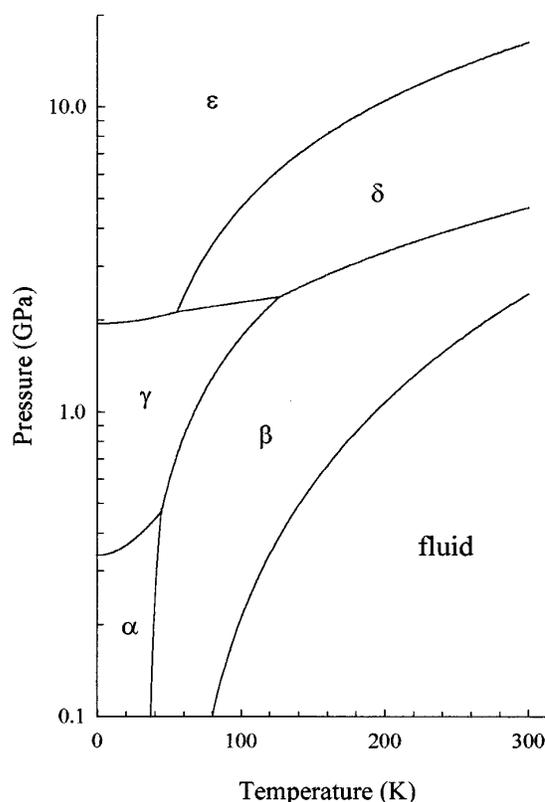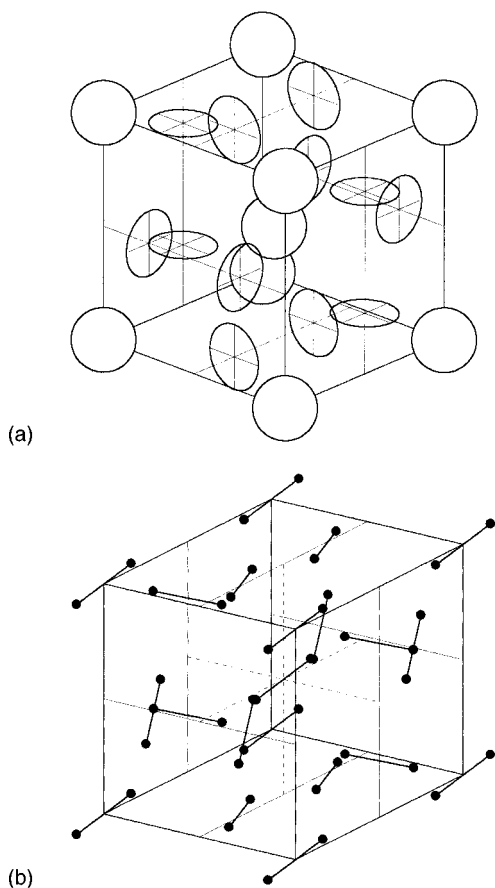

FIG. 1. Phase diagram of nitrogen.

(a)

(b)

FIG. 2. (a) δ-phase structure ($Pm3n$). (b) ε-phase structure ($R\bar{3}c$).

the delocalization process causes the break in the slope for ν_1. The localization has been mainly ascribed to the molecules at the sphere sites, the changes in the disk sites were supposed to be minor.

Orientational localization effects within the δ phase have also been observed with computer simulations. Nosé and Klein[20] studied the ε and δ phases at 7.0 GPa with constant-pressure molecular dynamics and a Lennard-Jones 12-6 atom-atom potential. This potential lacked a Coulomb term that reproduces the quadrupole moment of nitrogen. At decreasing temperature, the $Pm3n$ structure of the δ phase transformed at 230 K to a phase with $I2_13$ symmetry. In this
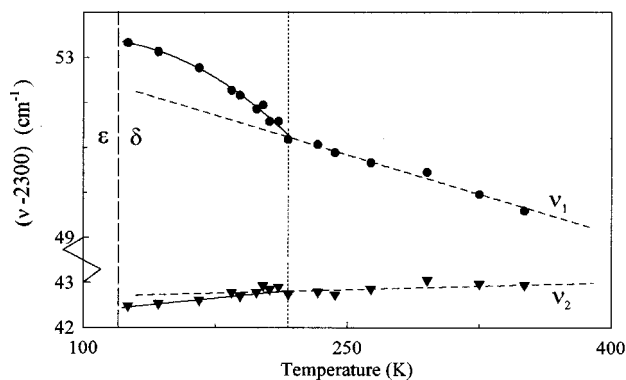
structure the molecules at the corners and the center of the unit cell are still spherically disordered, whereas the molecules in the faces of the cell take preferred orientations parallel to the unit-cell vectors. At 140 K this intermediate phase transformed to an orientationally ordered $R3c$ structure. However, the intermediate phase and the $R3c$ structure of the ε phase are not supported by experiments.

Belak and co-workers[17] have performed Monte Carlo simulations with a more sophisticated potential, the so-called Etters potential.[21] This potential consists of a site-site non-Coulomb part and an electrostatic or Coulomb part, which represents the quadrupole moment of nitrogen. Results obtained with this potential are very good: the properties of the dense fluid could be reproduced[22] and the α, β, and δ phase could be simulated.[17] Also, the ε-δ phase transition has been examined at 7.0 GPa.[17] As the temperature was decreased, a degree of orientational localization occurred at about 200 K, which increased with decreasing temperature. The $Pm3n$ symmetry was preserved to about 120 K; at this temperature the transition to an orientational ordered tetragonal phase occurred, which does not correspond to the experimental $R\bar{3}c$ structure of the ε phase. The difference in structure of the orientationally ordered phase obtained with the Lennard-Jones, and the Etters potential, is caused by the Coulomb term: Belak and co-workers[17] found that the neglect of the Coulomb term of the Etters potential resulted in the stability of the $R3c$ structure instead of the orientationally ordered tetragonal phase.

Although various properties could be calculated correctly with the Etters potential, the experimental ε- and γ-phase structure were not obtained. Therefore we have improved this potential by the addition of an anisotropic energy term,[23] which stabilizes the ε- and the γ-phase structure, next to the structures of the α, β, and δ phase. The new potential will be indicated below as the anisotropic potential. The details of this potential[23] and the results of the γ-β, α-γ, and α-β phase transitions[24] obtained with the anisotropic potential have been reported elsewhere.

In this work we will focus on the ε-δ phase transition and the orientational localization within the δ phase. We will present the results of Monte Carlo simulations with the anisotropic potential and the calculations of the Raman frequencies. Because the anisotropic energy term as well as the Coulomb term of the potential influence the orientational behavior, the effect of both terms on the orientation localization and the frequencies has also been examined.

II. METHOD

The (N,P,T) Monte Carlo method with the deformable simulation cell to study phase transitions has been described extensively in a previous paper.[23] The simulations of the γ-β and α-β phase transitions[24] have shown that orientational order-disorder behavior can be simulated easily. Although, in principle it is not impossible that the structural changes corresponding to these transitions can be simulated, due to the potential barrier these transitions did not occur with the usual simulation methods. Therefore, the ε-δ phase transition is very suitable for a complete study: next to the change in orientational behavior, the structural transition can be obtained merely by a change in simulation cell.[25]

FIG. 3. Frequency behavior of the nitrogen molecules in the δ and ε phase at 5.9 GPa, determined experimentally (Ref. 18).

The unit cell of the δ phase as well as the ε phase contains eight molecules, and the simulation cell was made up of four unit cells in each direction, resulting into a total of 512 molecules. In this way it was made sure that the dimensions of the boxlengths were larger than two times the cutoff range of the potential (9.0 Å). A cooling as well as a heating run, consisted of a number of successive (N,P,T) Monte Carlo simulations of 3000 equilibrium and 7000 production Monte Carlo steps (MCS). The final configuration of the simulation was used as the initial configuration for the next simulation. At the start of each run, the molecules of the ε-phase structure were given an orientation corresponding to the experimental structure [Fig. 2(b)]. Calculations have shown that these orientations are the most favorable.[23] The molecules of the δ phase were given a random orientation [Fig. 2(a)].

In order to study the orientational behavior of the molecules the orientational distribution functions (ODF's) were recorded in polar coordinates φ and $\cos\theta$, during the second part of the simulation. The orientational order parameters, which are based on the preferential orientations of the molecules, have been calculated through these ODF's.

The anisotropic potential consists of a site-site non-Coulomb part (core potential), an anisotropic energy term, and a Coulomb term formed by three point charges, resulting into a quadrupole moment of -4.7×10^{-40} C m^2. Next to the simulations with the anisotropic potential, we have performed simulations with the Etters potential, which does not only lack the anisotropic energy term, but has also a different Coulomb term, which is formed by four point charges, resulting in a quadrupole moment of -4.449×10^{-40} C m^2. Finally, simulations have been performed with the core potential, which lacks the anisotropic term as well as the Coulomb term.

The frequencies have been calculated as described by Michels and co-workers.[26] The frequency change, due to the intermolecular forces, was calculated through a first- and second-order effect. The first-order effect is caused by the external forces, exerted by the surrounding molecules on the sites of the molecule. Although the molecules have been regarded as rigid rotors, the resulting axial force, F_{ax} would result in a change in the equilibrium bond length. The resulting change of vibrational frequency was calculated by

$$\Delta\omega_1 = c_1 F_{ax}, \tag{1}$$

with

$$c_1 = 3.807\times10^{10} \text{ N}^{-1}\text{ cm}^{-1}.$$

The external force will not be homogeneous; F_{ax} will depend on the bond length r. This second-order effect of the frequency change was calculated by

$$\Delta\omega_2 = c_2 f', \tag{2}$$

with

$$c_2 = 0.507 \text{ N}^{-1}\text{ m cm}^{-1}.$$

The derivative f' was determined by the differential

$$f' \approx \frac{\Delta F_{ax}(r)}{\Delta r} = \frac{F_{ax}(r+\Delta r) - F_{ax}(r-\Delta r)}{2\Delta r} \tag{3}$$
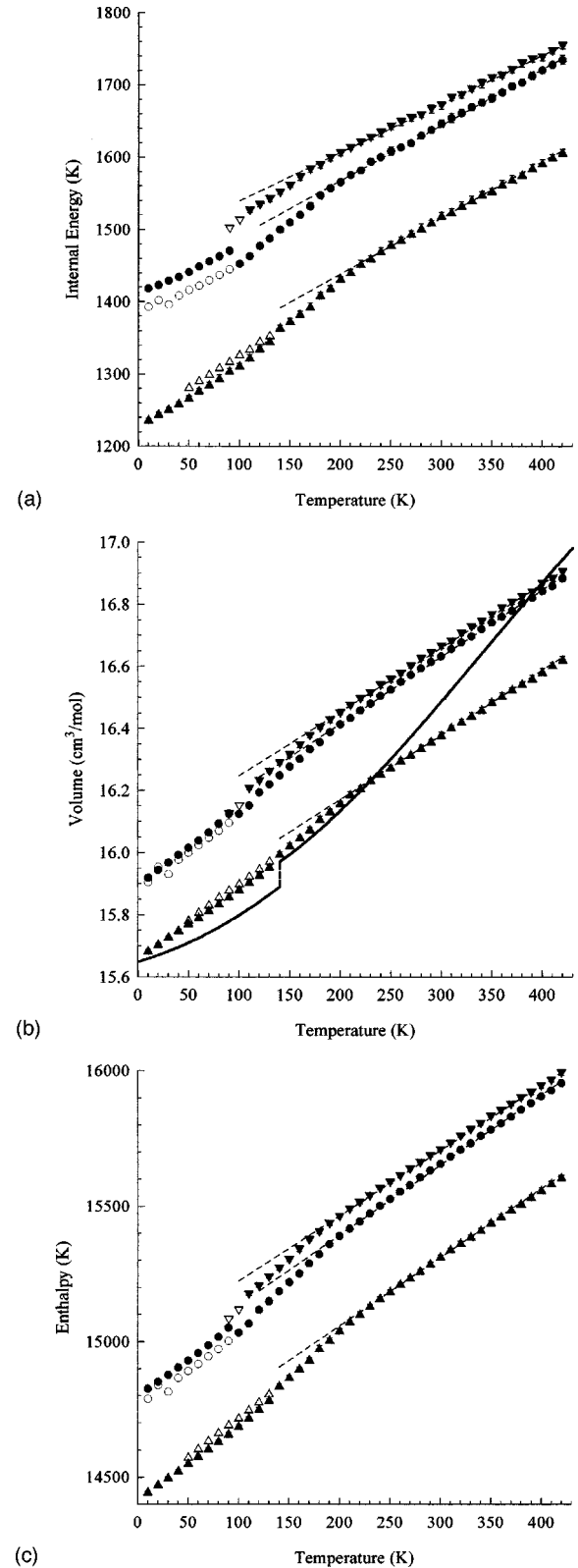

(a)

(b)

(c)

FIG. 4. (a) Energy, (b) volume, and (c) enthalpy as a function of temperature of the heating run (closed symbols) and the cooling run (open symbols) at 7.0 GPa. The results obtained with the anisotropic potential are indicated by an up triangle, the Etters potential by a dot, and the core potential by a down triangle. The thick solid line originates from the V-T diagram of the experimental data of Mills and co-workers (Ref. 11).
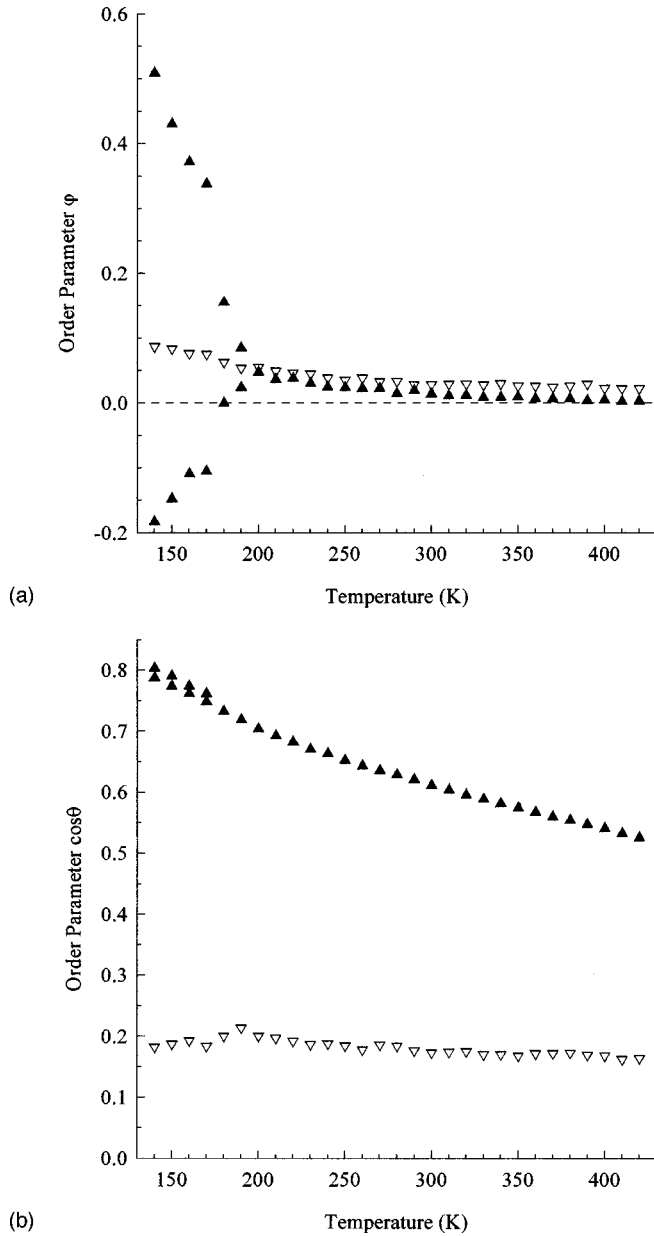
(a)

(b)

FIG. 5. Orientational order parameter of the molecules at the sphere sites (open triangles) and the disk sites (closed triangles) as a function of temperature of (a) the φ coordinate and (b) the $\cos \theta$ coordinate, obtained with the anisotropic potential.

for each molecule, while all other molecules were kept at their positions. For Δr a value of 0.005×10^{-10} m was taken.

The momentary forces acting on the sites have been calculated after each MCS, and although the simulations have been performed with the anisotropic, Etters, or core potential, the forces were calculated in each case through the core potential, which lacks the anisotropic energy and Coulomb term. This method of frequency calculation does not take into account vibration-rotation coupling, resonance coupling, and bond-length dependence of the potential.

The resulting vibration frequency of each molecule is given by

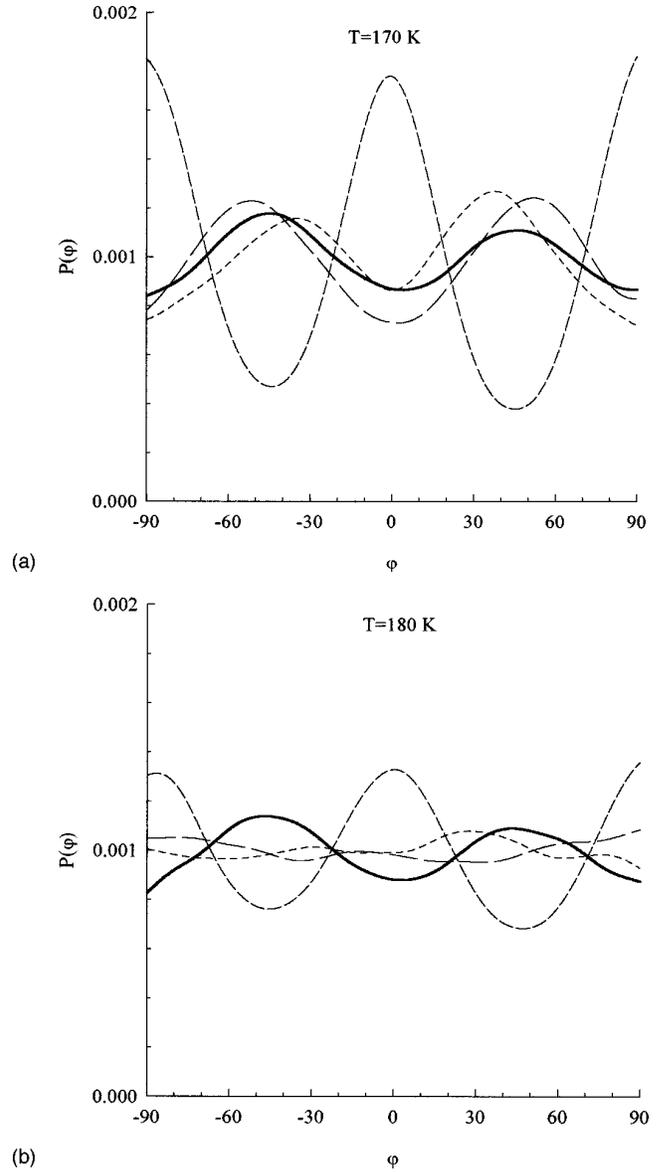$$\omega = \omega_0 + \Delta \omega_1 + \Delta \omega_2, \tag{4}$$

(a)

(b)

FIG. 6. The ODF of the φ coordinate at (a) 170 K and (b) 180 K obtained with the anisotropic potential. The solid line indicates the ODF of the sphere sites and the dashed lines of the disk sites.

with ω_0 the frequency of an isolated, nonrotating molecule. For both phases, the frequency change of the molecules at the spherical sites, as well as those at the disk sites at the same face, have been averaged separately, leading to four frequency values.

III. RESULTS

A. The anisotropic potential

The ε-δ phase transition and the second-order effect have been examined at 7.0 GPa with the anisotropic potential. For this purpose a heating run has been performed from 10 to 420 K in steps of 10 K, starting with the experimental ε-phase structure. The energy, volume, and enthalpy of this heating run are given in Figs. 4(a), 4(b), and 4(c), respectively. Up to 130 K the ε phase continued to exist. The
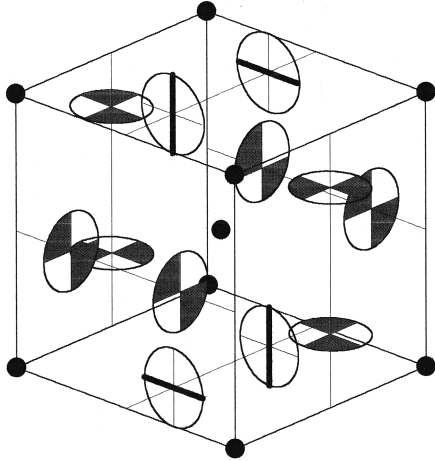
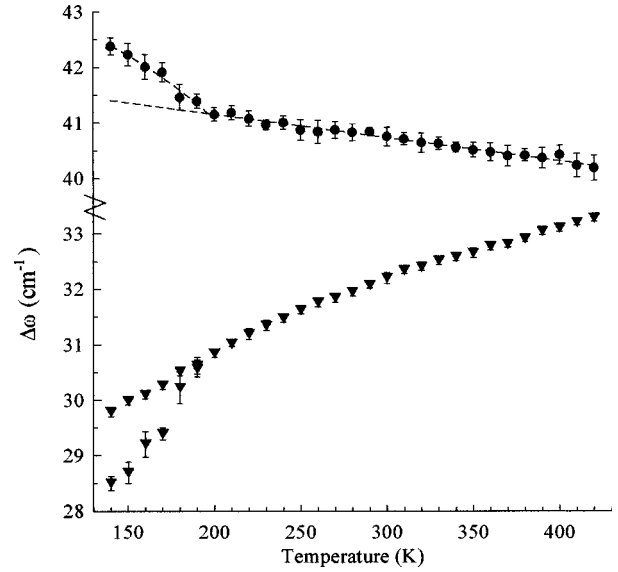FIG. 7. Preferential orientation of the molecules; see text.

FIG. 8. The change of the vibrational frequency of the molecules at the sphere sites (dots), and the disk sites (triangles) as a function of temperature, obtained with the anisotropic potential.

transition to the δ phase occurred between 130 and 140 K, and has been observed by a jump in energy, volume, and enthalpy, a change in the box angle of the simulation cell from about 85° to 90° and in the orientational behavior of the molecules.

Besides, a cooling run has been performed; starting at 140 K the temperature was lowered in steps of 10 K. The final configuration of the heating run at 140 K has been used as the initial configuration. The results of these simulations are also given in Figs. 4(a)–4(c). Although the ε phase transformed to the δ phase, the transition from the δ to the ε phase did not occur; the δ phase continued to exist below 140 K. The volume change of the ε-δ phase transition is about 0.02 cm^3/mol The energy as well as the volume of the ε phase is lower than that of the δ phase. The second-order phase transition within the δ phase, which is probably caused by orientation localization, could be detected by a change in the thermal expansion, the orientational order parameters, and the frequency.

From Fig. 4(b) it can be seen that the thermal expansion $\Delta V/\Delta T$ changes within the δ phase: from 0.21 $\times 10^{-2}$ cm^3/mol K at high temperature to 0.26 $\times 10^{-2}$ cm^3/mol K below 200 K. Apparently, because the $Pm3n$ symmetry of the lattice positions of the δ-phase structure is preserved, the larger compressibility is caused by a change in orientational behavior. A comparable effect has been found by Olijnyk[12] who performed pV measurements at room temperature using x-ray diffraction. At higher pressures a softening of the isotherm was found that could be explained by an increase in compressibility caused by orientational localization.

Although the orientational behavior of the molecules at the disk and sphere sites at high temperature is highly dynamical, both sites exhibit weakly preferred orientations. The molecules at the disk sites prefer to align along the axis within the face, and perpendicular to the face ($\varphi=0°$, 90°; $\cos\theta=0$), and the molecules at the sphere sites along the four body diagonals ($\varphi=\pm 45°$; $\cos\theta=\pm\frac{1}{3}\sqrt{3}$). Based on these preferential orientations, the orientational order parameters of the sphere sites are defined as

$$O_s^\varphi = \cos[4(\varphi - 45°)],$$

$$O_s^{\cos\theta} = \cos[\sqrt{3}\,\pi(\cos\theta - \tfrac{1}{3}\sqrt{3})], \tag{5}$$

and of the disk sites as

$$O_d^\varphi = \cos(4\varphi),$$

$$O_d^{\cos\theta} = \cos(\pi\cos\theta). \tag{6}$$

The order parameters as a function of temperature are given in Fig. 5. The δ phase at high temperature is called δ_{rot}, since the orientational behavior of the molecules is highly dynamical. The preferred orientations of the sphere and the disk sites become more pronounced with decreasing temperature; the order parameters increase. Above 190 K the orientational distribution functions of the three disk sites are equal, and the order parameters are averaged for clarity. Although the increase in the order parameters continues gradually for the sphere sites, the behavior of the order parameter of the φ coordinate of disk sites changes dramatically below 200 K. The order parameter of one disk site increases rapidly, whereas that of the other two disk sites decreases and becomes negative. This behavior can be explained on the basis of the ODF given in Fig. 6. Below 200 K, the preferred orientations at $\varphi=0°$ and 90° of one of the disk sites become more pronounced rapidly, whereas that of the other two disk sites disappear. Moreover, below 180 K the preferred orientations of these two disk sites change to $\varphi\approx\pm 35°$ and $\varphi\approx\pm 50°$, which causes the order parameter to be negative. Note the rapid change in order parameter for all disk sites between 170 and 180 K [Fig. 5(a)]. The molecules that are localized at $\varphi=0°$ and 90° are slightly more located within the plane as can be observed by the $\cos\theta$ order parameter. A small shift ($\cos\theta$ to about ± 0.5) can be observed for the preferential orientations of the sphere sites; as an effect the order parameter becomes slightly lower. On further cool-
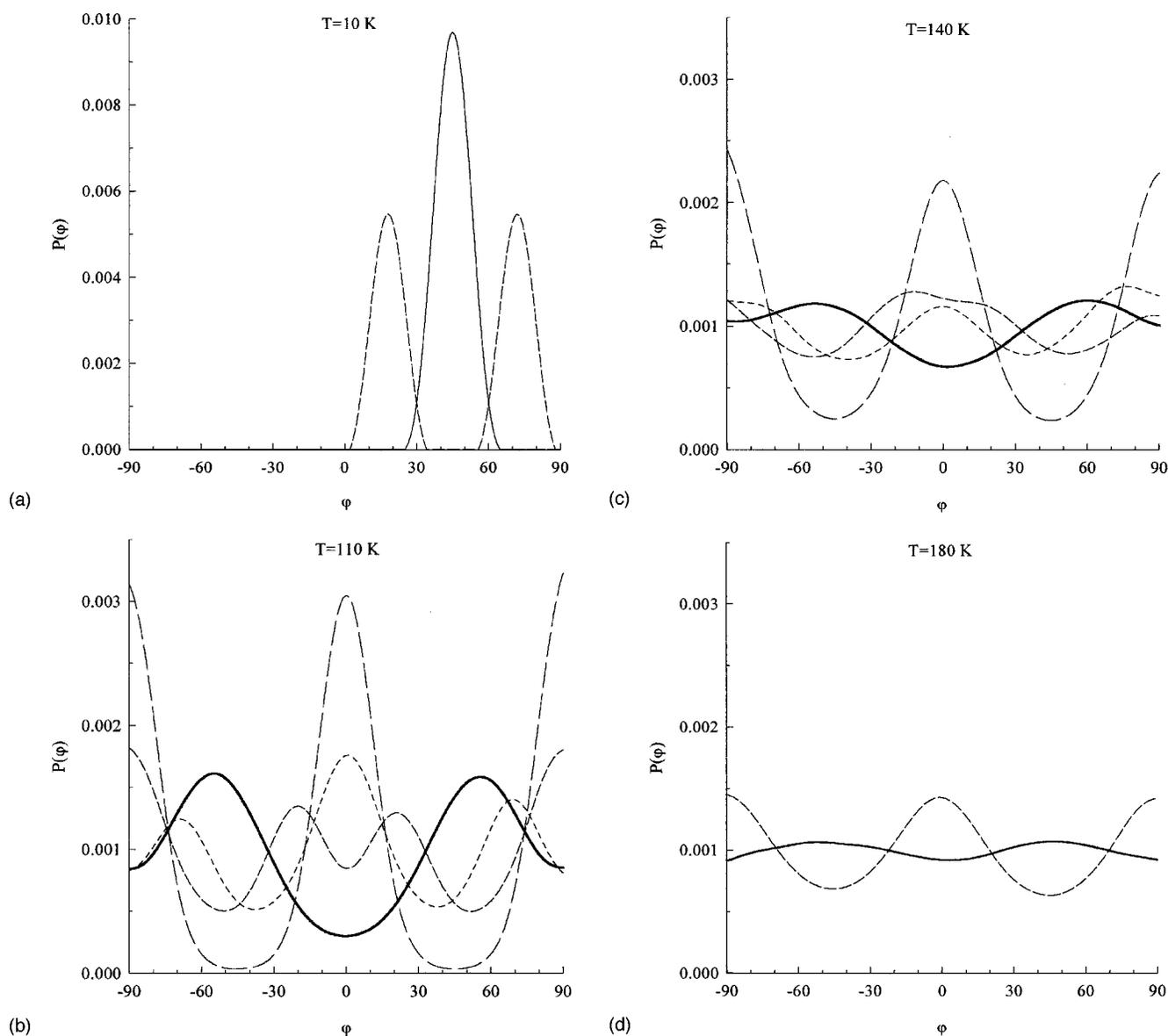
FIG. 9. The ODF of (a) the $R3c$ structure at 10 K, the tetragonal structure at (b) 110 K and (c) 140 K, and (d) the cubic structure at 180 K, obtained with the Etters potential. The solid line indicates the ODF of the sphere sites and the dashed lines of the disk sites.

ing, the ODF revealed a gradual splitting of the orientations at $\varphi \approx \pm 35°$ and $\varphi \approx \pm 50°$, from about 60 K below the ε-δ phase transition temperature.

The change of preferential orientations in combination with localization causes the second-order transition within the δ phase in this model system. Investigation of the degree of localization revealed that the molecules at the spherical sites, although the orientations along the body diagonals are preferred, are not localized. On the other hand, the molecules at the disk sites, are localized and librate along one direction. This orientational localized δ-phase structure is called δ_{loc}. The orientation of the molecules has been investigated in the δ_{loc} phase at 140 K and at about 7 GPa. Consider the disks in a line along one of the unit vectors of the unit cell. The disks with an orientation distribution function showing preferential orientations at $\varphi = 0°$ and $\varphi = 90°$ have alternately $\varphi = 0°$ or $\varphi = 90°$ along the line. This holds for all three directions. In the case of the other two types of disks alternately two disks have $\varphi = -35°$ (or $-50°$) and two disks have $\varphi = 35°$ (or $50°$) in one of the directions. In another direction the orien-

tation of all the molecules is the same while in the third direction the disks have alternately $\varphi = 35°$ $(50°)$ or $\varphi = -35°$ $(-50°)$. As a result there are also correlations between the orientation of the disks in two different lines with the same as well as with different directions. The unit cell consists of 64 molecules. The situation is partly depicted in Fig. 7.

The time behavior of the individual molecules has also been studied. A certain disk molecule is librating around its own preferential orientation, the angle of libration can be observed from the ODF. There is a small chance that the orientation is temporarily close to the preferential orientation of a neighboring molecule in the same line but this holds only for a small time and the molecule flips back to its original orientation. There is no indication that the orientation of a molecule on a sphere position is related to that of its neighbors.

The box lengths and the box angles are the same in the δ_{loc} and the δ_{rot} phase, within the accuracy of the calculations. Also the average position of the molecules at the disks
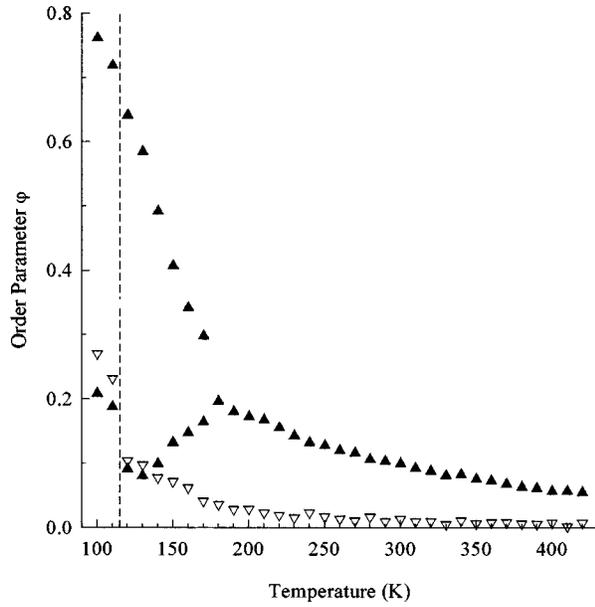
(a)
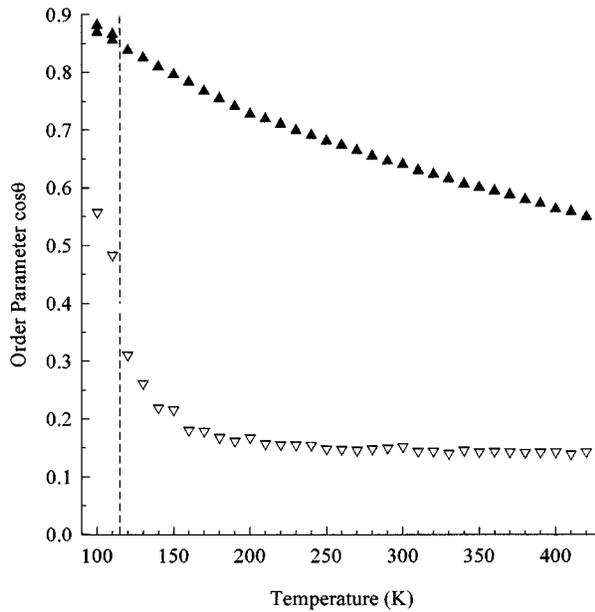
(b)

FIG. 10. The order parameter of the molecules at the sphere sites (open triangles) and the disk sites (closed triangles) as a function of temperature of (a) the φ coordinate and (b) the $\cos\theta$ coordinate, obtained with the Etters potential.

as well as the sphere sites is the same below and above the second-order transition. It is possible that the deviation is too small to be detected. Therefore, we have also performed simulations with the cubic unit cell with fixed box lengths and fixed box angles. It turned out that there is no difference compared to the results obtained using a variable box.

One might anticipate that the change in the orientational behavior of the molecules at the *disk* sites below 200 K influences the frequency of the molecules at the *sphere* sites, because the vibrational frequency of a molecule depends on the behavior of the surrounding molecules. The frequency shift of the sphere (ν_1) and disk sites (ν_2) as function of temperature is given in Fig. 8. Indeed, although hardly no change in orientational behavior of the sphere sites is observed, the frequency behavior changes below 200 K, which is a consequence of the change in orientational behavior of
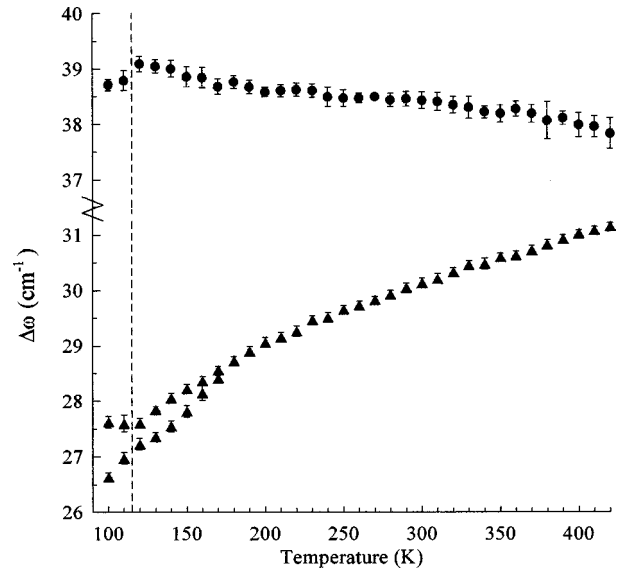

FIG. 11. The change of the vibrational frequency of the molecules at the sphere sites (dots), and the disk sites (triangles) as a function of temperature, obtained with the Etters potential.

the molecules at the disk sites. Simultaneously, the frequency of the molecules at the disk sites split: the frequency of the molecules with preferential orientations at $\varphi = 0°$ and 90° is about 1 cm^{-1} lower than the frequency of the molecules with preferential orientations at $\varphi \approx \pm 35°$ and $\varphi \approx \pm 50°$.

B. The Etters potential

In order to examine the influence of the anisotropic part of the potential on the orientational behavior of the molecules in the δ phase, we have performed simulations with the original Etters potential, which lacks the anisotropic energy part. The calculations have been performed in the same way as the calculations of the previous section: starting with the experimental ε-phase structure the temperature is increased from 10 to 420 K in steps of 10 K. The resulting volume, energy and enthalpy vs temperature at 7.0 GPa are given in Fig. 4.

At 10 K, the $R\bar{3}c$ initial configuration, which was stabilized by the anisotropic potential, relaxed to a $R3c$ structure [Fig. 9(a)] with box angles of about 85.6°, which transformed to a tetragonal structure [Fig. 9(b)] above 90 K with box lengths $a=b\neq c$. Above 110 K the tetragonal structure transformed to the δ-phase structure. Besides, a cooling run was performed by decreasing the temperature in steps of 10 K, using the tetragonal structure at 110 K as the initial configuration at 100 K. The tetragonal structure continued to exist down to 10 K (Fig. 4). These results are in agreement with the results obtained by Belak and co-workers.[17] Note that the $R3c$ structure exhibits a higher enthalpy than the tetragonal structure, in contrast with the calculations with the anisotropic potential for which the enthalpy of the $R\bar{3}c$ structure is lower than that of the δ_{loc} structure.

The calculated order parameters, which are defined as before, and frequency vs temperature are given in Figs. 10 and 11, respectively. If the temperature is decreased, the order
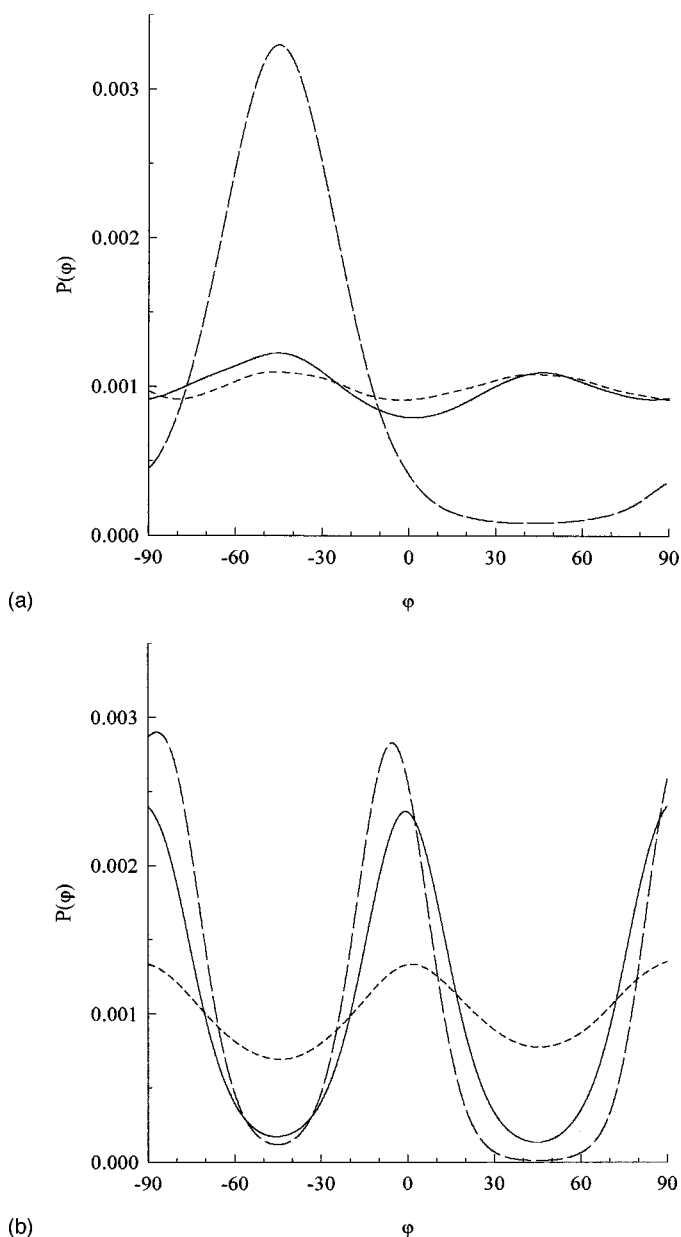
(a)

(b)

FIG. 12. The ODF for (a) the molecules at the sphere sites, and (b) the disk sites at 100 (long dashed), 110 (solid) and 200 (short dashed) K, obtained with the core potential.

parameter of the φ coordinate of the molecules at the sphere and the disk sites increases. The preferential orientations of the molecules at the disk sites are more pronounced than that of the sphere sites and persist to very high temperature: at room temperature the order parameter is still about 0.1. Below 180 K the orientational behavior of the molecules change: the order parameter of the molecules at the sphere sites increases more rapidly, and the order parameter of the molecules at the disk sites split. As with the calculations with the anisotropic potential, for one of the disk sites the preferential orientations at 0° and 90° become more pronounced. The other two disk sites show a different behavior in which the preferential orientation at 0° or 90° gradually split about 40° between 110 and 180 K, in course of which the order parameter decreases, but not to negative values. This behavior is depicted by the ODF in Fig. 9. As a consequence of the difference in orientational behavior, the frequency of the
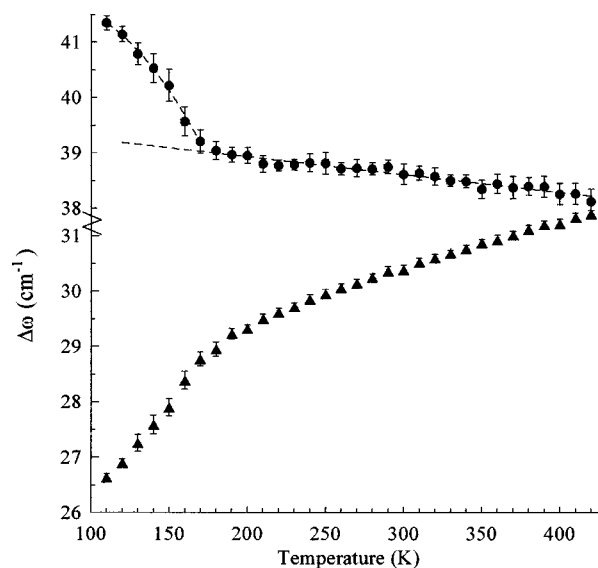

FIG. 13. The change of the vibrational frequency of the molecules at the sphere sites (dots), and the disk sites (triangles) as a function of temperature, obtained with the core potential.

molecules at the disk sites split with a maximum difference of about 0.5 cm^{-1}. The molecules with the preferential orientations at 0° and 90° have a lower frequency. The change in orientational behavior of the molecules at the disk sites does not noticeably influence the frequency of the molecules at the sphere sites, in contrast with the experimental results.

Below 120 K the δ-phase transforms to the tetragonal structure and the preferred orientations become much more pronounced. As an effect the frequency splitting increases up to about 2.3 cm^{-1} at 10 K. This frequency splitting of the tetragonal phase was also suggested by the simulations of Belak and co-workers.[17] The box length with the smaller value corresponds to the disk sites for which the molecules align at 0° and 90° and have the higher frequency.

C. The core potential

The quadrupole moment of the Etters and the anisotropic potential are slightly different: -4.9×10^{-40} C m^2 and -4.4×10^{-40} C m^2, respectively. Although calculations showed that this difference in quadrupole moment did not influence the second-order effect, it is interesting to examine the second-order effect without the Coulomb term. Therefore we have performed simulations with a potential that lacks the anisotropic part as well as the Coulomb part: the core potential. Starting with the δ-phase structure, the temperature was decreased from 420 to 90 K in steps of 10 K. The resulting volume, energy, and enthalpy vs temperature are given in Fig. 4. The δ-phase structure continued to exist until 100 K, at which temperature it transformed to a $R3c$ structure with box angles of about 87.4°. This structure corresponds to the structure obtained by Nosé and Klein.[20] The orientational ordering of this structure differs from that of the $R3c$ structure obtained with the Etters potential. The orientational behavior of the molecules at 100, 110, and 220 K is depicted by the ODF in Fig. 12. The frequency and order parameter, defined as before, vs temperature are shown in Figs. 13 and 14, respectively.
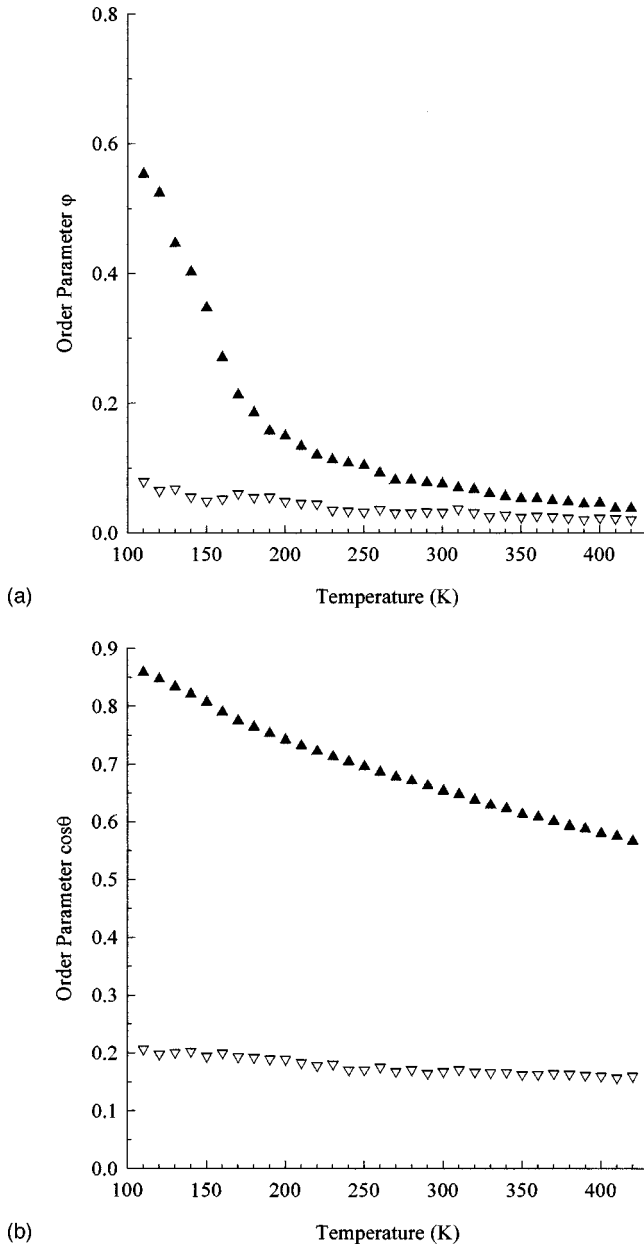
(a)

(b)

FIG. 14. The order parameter of the molecules at the sphere sites (open triangles) and the disk sites (closed triangles) as a function of temperature of (a) the φ coordinate and (b) the $\cos \theta$ coordinate, obtained with the Etters potential.

As with the calculations with the Etters and the anisotropic potential, the orientational behavior of the molecules at the sphere sites hardly changes with temperature. The preferential orientations of the molecules at the disk sites are more pronounced than that of the sphere sites, and the order parameter increases with decreasing temperature. Below 190 K the orientations of the molecules of the disk sites become rapidly more localized, whereas the preferential orientations, which are the same for all three disk sites, do not change. As a result, the frequency of the sphere sites increase rapidly below 190 K. Although this frequency behavior resembles the behavior of the frequency found with the anisotropic potential, the orientational behavior is different. Also the rate of decrease in frequency of the molecules at the disk sites increases below 190 K, and is equal for the three different sites, because the orientational behavior is identical.

TABLE I. Coefficients of Eq. (7) of the fits of $(\nu_1 - \nu_2)$ vs the temperature at 7.0 GPa for the $\delta_{\rm rot}$ structure obtained with the anisotropic, Etters, and core potential between 200 and 420 K, and the experimentally determined values (Ref. 19).

	b_0 (cm^{-1})	b_1 (cm^{-1}/K)
Anisotropic potential	13.09	-0.01489
Etters potential	12.07	-0.01266
Core potential	11.96	-0.01244
Expt.	12.61	-0.01349

IV. DISCUSSION AND CONCLUSION

The ε-δ phase transition and the second-order transition within the δ phase have been examined at 7.0 GPa with Monte Carlo simulations and the recently developed potential. The ε phase transformed to the δ phase between 130 and 140 K, in agreement with experiment.[11] The volume change $\Delta V(\delta$-$\varepsilon)$ of about 0.1% is smaller than the experimental value of 0.5% obtained by Mills and co-workers.[11] The volume of the ε phase is a few tenths of a percent off compared with the experimental data of Mills and co-workers;[11] the volume of the δ phase differs about 0.1% at low temperature, and about 2% at high temperature. The volume of the ε phase calculated with the Etters and the core potential is about 2% too high. The same holds for the δ phase at low temperatures; at high temperature the agreement is much better.

Investigation of the orientational behavior of the molecules revealed that below 190 K the δ-phase structure is orientationally ordered. This so-called $\delta_{\rm loc}$ structure remained stable below 140 K, and at temperatures below 90 K the orientational order becomes more exotic. Since the $\delta_{\rm loc}$ structure has a larger enthalpy than the ε-phase structure, it is likely to be metastable. Apparently, the transition involves a potential barrier that is too large to overcome; an effect that has also been observed with the simulation of the α, β, and γ phases.

The behavior of the calculated frequencies within the δ-phase region resembles the experimental behavior. Scheerboom and Schouten[18] ascribed this behavior to a cascade process in which the molecules, orientationally localized just at the ε-δ transition, obtain rapidly more orientational freedom at increasing temperature. The end of the delocalization process causes a break in the frequency slope for ν_1. The simulations of the model system revealed that the process is more complicated. Indeed, at the structural ε-δ phase transition the δ phase is orientationally localized, but this localization holds only for the molecules at the *disk* sites; the molecules at the sphere sites still rotate more or less freely. On increasing the temperature the librations at the disk sites increase, which influences the frequency of the molecules at the sphere sites, but the molecules at the disk sites remain orientationally ordered. Above 170 K the localization vanishes, accompanied by a change in preferential orientations of the molecules at the disk sites. The splitting of the frequency of the molecules at the disks sites at low temperature, caused by the difference in localization, has not been reported in Ref. 18. This might be due to the experimental resolution, but needs further investigation. The intensity of

the two frequencies would be 1:2 (low:high), because the molecules with the preferential orientations at $\varphi \approx \pm 35°$ and $\varphi \approx \pm 50°$ exhibit the same frequency. We have also examined the effect of the anisotropic and the Coulomb term on the orientational localization within the δ phase. Therefore three potentials have been used: the core potential, which lacks the anisotropic energy term as well as the Coulomb term, the Etters potential, which lacks the anisotropic energy term, and the anisotropic potential.

The frequency difference $\nu_1 - \nu_2$ of the δ_{rot} structure can be described by a linear expression:[19]

$$(\nu_1 - \nu_2) = b_0 - b_1 T. \qquad (7)$$

The coefficients of the fits through the data of the anisotropic, Etters, and core potential, next to the experimentally[19] determined coefficients, are given in Table I. Although the difference in coefficients is small, the results obtained with the Etters and anisotropic potential are in better agreement with experiment. The Coulomb term as well as the anisotropic energy term have no influence on the orientational behavior of the molecules at the sphere sites: the preferential orientations gradually increase with decreasing temperature, while no localization occurs.

All three potentials reveal orientational localization of the molecules at the disk sites, though the nature of the localization is different. The preferential orientations at high temperature of the molecules at the disk sites are identical for all the potentials, but are much more pronounced when the intermolecular potential lacks the anisotropic energy term. In case of the core potential, these preferential orientations become rapidly more pronounced below 200 K, which causes a change in the frequency behavior of the molecules at the

spherical sites. The addition of the Coulomb term (the Etters potential) causes the direction of the preferential orientations to change below 180 K. Because this change is small and occurs *gradually* between 110 and 190 K, there is no noticeable influence on the frequency behavior of the molecules at the sphere sites, in contrast with experiment. The anisotropic energy term, on the other hand, causes an *unambiguous* change of the preferential orientations at 170 K, which causes a change in the frequency behavior of the molecules at the spherical sites, corresponding to the experimental observations.

Independent of the potential, the preferential orientation at 0° and 90° of at least one of the disk sites become rapidly more pronounced for the δ_{loc} structure. It is this disk site that has the lower frequency and for which the change in the frequency behavior is the largest. The increase in order parameter of this disk site is smallest in the case of the core potential, but it occurs for all disk sites, resulting in the largest change in frequency behavior of the sphere sites.

Scheerboom and Schouten[18] observed that the linear behavior of ν_2 of the δ_{loc} structure is slightly steeper than that of the δ_{rot} structure (Fig. 3). If the calculated frequencies of the three disk sites are averaged, this behavior can be observed for all three potentials, but is too large in case of the core potential.

Although the frequency behavior of the sphere sites obtained with the core potential and the anisotropic potential resembles the experimental behavior, only the latter includes an expression for the quadrupole moment of nitrogen and stabilizes the experimental ε-phase structure. Experiments have to be performed, which can measure the Raman frequency accurately, to confirm the splitting of the ν_2 frequency of the δ_{loc} phase.

[1] W. E. Streib, T. H. Jordan, and W. N. Lipscomb, J. Chem. Phys. **37**, 2962 (1962).

[2] T. H. Jordan, H. W. Smith, W. E. Streib, and W. N. Lipscomb, J. Chem. Phys. **41**, 756 (1964).

[3] A. F. Schuch and R. L. Mills, J. Chem. Phys. **52**, 6000 (1970).

[4] D. Schiferl, D. T. Cromer, and R. L. Mills, High Temp.-High Press. **10**, 493 (1978).

[5] D. Schiferl, D. T. Cromer, R. R. Ryan, A. C. Larson, R. LeSar, and R. L. Mills, Acta Crystallogr., Sect. C: Cryst. Struct. Commun. **39**, 1151 (1983).

[6] C. A. Swenson, J. Chem. Phys. **23**, 1963 (1955).

[7] L. H. Bolz, M. E. Boyd, F. A. Mauer, and H. S. Peiser, Acta Crystallogr. **12**, 247 (1959).

[8] E. M. Hörl and L. Marton, Acta Crystallogr. **14**, 11 (1961).

[9] J. A. Venables and C. A. English, Acta Crystallogr., Sect. B: Struct. Crystallogr. Cryst. Chem. **30**, 929 (1974).

[10] R. L. Mills and A. F. Schuch, Phys. Rev. Lett. **23**, 1154 (1969).

[11] R. L. Mills, B. Olinger, and D. T. Cromer, J. Chem. Phys. **84**, 2837 (1986).

[12] H. Olijnyk, J. Chem. Phys. **93**, 8968 (1990).

[13] M. I. M. Scheerboom and J. A. Schouten, J. Phys.: Condens. Matter **3**, 8305 (1991).

[14] H. Schneider, W. Häfner, A. Wokaun, and H. Olijnyk, J. Chem. Phys. **96**, 8046 (1992).

[15] D. T. Cromer, R. L. Mills, D. Schiferl, and L. A. Schwalbe, Acta Crystallogr., Sect. B: Struct. Crystallogr. Cryst. Chem. **37**, 8 (1981).

[16] M. L. Klein, D. Levesque, and J. J. Weis, Can. J. Phys. **59**, 530 (1981).

[17] J. Belak, R. LeSar, and R. D. Etters, J. Chem. Phys. **92**, 5430 (1990).

[18] M. I. M. Scheerboom and J. A. Schouten, Phys. Rev. Lett. **71**, 2252 (1993).

[19] M. I. M. Scheerboom and J. A. Schouten, J. Chem. Phys. **105**, 2553 (1996).

[20] S. Nosé and M. L. Klein, Phys. Rev. Lett. **50**, 1207 (1983).

[21] R. D. Etters, V. Chandrasekharan, E. Uzan, and K. Kobashi, Phys. Rev. B **33**, 8615 (1986).

[22] J. Belak, R. D. Etters, and R. LeSar, J. Chem. Phys. **89**, 1625 (1988).

[23] A. Mulder, J. P. J. Michels, and J. A. Schouten, J. Chem. Phys. **105**, 3235 (1996).

[24] A. Mulder, J. P. J. Michels, and J. A. Schouten, J. Chem. Phys. **106**, 8806 (1997).

[25] B. Kutchta, K. Rohleder, R. D. Etters, and J. Belak, J. Chem. Phys. **102**, 3349 (1995).

[26] J. P. J. Michels, M. I. M. Scheerboom, and J. A. Schouten, J. Chem. Phys. **103**, 8338 (1995).